IEEE Access
Multidisciplinary | Rapid Review | Open Access Journal

Received December 10, 2019, accepted December 17, 2019, date of publication December 23, 2019,
date of current version January 6, 2020.

Digital Object Identifier 10.1109/ACCESS.2019.2961740

A Localization Based on Unscented Kalman Filter and Particle Filter Localization Algorithms

INAM ULLAH[1], YU SHEN[1], XIN SU[1], (Senior Member, IEEE), CHRISTIAN ESPOSITO[2], AND CHANG CHOI[3], (Senior Member, IEEE)

[1]College of Internet of Things (IoT) Engineering, Hohai University (HHU), Changzhou Campus, Changzhou 213022, China
[2]Department of Computer Science, University of Salerno, 84084 Fisciano, Italy
[3]Department of Computer Engineering, Gachon University, Seongnam 13120, South Korea

Corresponding author: Chang Choi (enduranceaura@gmail.com)

This work was supported in part by the National Natural Science Foundation of China under Grant 61801166, in part by the Fundamental Research Funds for the Central Universities under Grant 2019B22214, in part by the National Research Foundation of Korea (NRF) grant funded by the Korea government (Ministry of Science and ICT) under Grant 2017R1E1A1A01077913, and in part by the Global Infrastructure Program through the National Research Foundation of Korea (NRF) funded by the Ministry of Science and ICT under Grant NRF-2018K1A3A1A20026485.

ABSTRACT Localization plays an important role in the field of Wireless Sensor Networks (WSNs) and robotics. Currently, localization is a very vibrant scientific research field with many potential applications. Localization offers a variety of services for the customers, for example, in the field of WSN, its importance is unlimited, in the field of logistics, robotics, and IT services. Particularly localization is coupled with the case of human-machine interaction, autonomous systems, and the applications of augmented reality. Also, the collaboration of WSNs and distributed robotics has led to the creation of Mobile Sensor Networks (MSNs). Nowadays there has been an increasing interest in the creation of MSNs and they are the preferred aspect of WSNs in which mobility plays an important role while an application is going to execute. To overcome the issues regarding localization, the authors developed a framework of three algorithms named Extended Kalman Filter (EKF), Unscented Kalman Filter (UKF) and Particle Filter (PF) Localization algorithms. In our previous study, the authors only focused on EKF-based localization. In this paper, the authors present a modified Kalman Filter (KF) for localization based on UKF and PF Localization. In the paper, all these algorithms are compared in very detail and evaluated based on their performance. The proposed localization algorithms can be applied to any type of localization approach, especially in the case of robot localization. Despite the harsh physical environment and several issues during localization, the result shows an outstanding localization performance within a limited time. The robustness of the proposed algorithms is verified through numerical simulations. The simulation results show that proposed localization algorithms can be used for various purposes such as target tracking, robot localization, and can improve the performance of localization.

INDEX TERMS Extended Kalman filter, localization, particle filter, robot, unscented Kalman filter, wireless sensor networks.

I. INTRODUCTION

The applications of Wireless Sensor Networks (WSNs) are used widely for various purposes such as environmental monitoring (air, oil, temperature or soil quality), traffic monitoring, smart industries applications, and intelligent transport systems. Normally, wireless nodes are small low-power sensors over a few tens of a square area. The information is transformed between sensor nodes in the form of packets and receives meaningful information [1], [2]. The sensor nodes are required to be located. Although GPS achieves a power localization, it is unfeasible and expensive to fit every sensor node in a WSN along with a GPS maneuver. The WSNs applications [3], [4] required an exact node position that needs an efficient localization approach. In the past, all the localization approaches are based on very fine numerical computation of numerous network parameters. These parameters include the power of transmission or receiving,

The associate editor coordinating the review of this manuscript and approving it for publication was Ilsun You.

shape of the propagation, connectivity information, transmission range, time of the transmission and reception, etc. These constraints are likely towards environmental conditions and environmental complications. Most of the recent research work in the area of localization focuses on the minimization of localization errors during localization [5]–[7].

Unscented Kalman Filter (UKF) relates to the class of Sigma-Point Kalman Filters (SPKF) or Linear Regression Kalman Filters (LRKF), which usually use the method of statistical linearization. UKF is applied to linearize the random variable non-linear functions by applying the linear regression among n points which is derived from the previous distribution of the random variables. In EKF, the state distribution is spread systematically by the first order linearization of the non-linear system, resultantly corrupt the posterior covariance and mean. Alternatively, applying UKF, which is derivative-free, solves this issue by applying the sampling approach of deterministic. A minimal set of selected sample points are selected to represent the state distribution, known as sigma points. Similar to the EKF, UKF also applying the two same stages such as model forecast and data assimilation. UKF is based on the perception that it is relaxed to estimate a probability distribution that is to estimate a random non-linear function. The sigma points are selected so that their mean and covariance will be x^a_{k-1} and P_{k-1} [8]. Every sigma point is then broadcasted by the nonlinearity yielding, in the end, a transformed point in the form of a cloud. The innovative estimated mean and covariance are then calculated based on their statistics. The unscented transform is a method for estimating the statistics of a random variable which experiences a non-linear transformation. Let us consider a non-linear system defined by the model of state x_k transition and observation.

$$x_k = f(x_{k-1}, u_k) + w_k \tag{1}$$
$$z_k = h(x_k) + v_k \tag{2}$$

where the function f is to calculate the predicted state from the prior estimated state and h can be used to determine the previously expected calculation. However, f and h cannot be used directly for the covariance, instead, a partial derivative (Jacobian) matrix is calculated. At every step, the Jacobian is estimated with the existed predicted state and these matrices can be applied for the equations of Kalman Filter (KF). This method effectively linearizes the non-linear equation around the current estimate, which is EKF's fundamental principle.

A particle's basic concept is to make a different sum of assumptions about the likely position of the robot, each of which is known as a particle. Particle observes and travels similar to the robot and perform as a cybernetic copy of the robot. But particle does not perform in real, while with the help of the map of the surrounding. As the particle precision agrees with the robot, the probability increase that the particle is near to the position of the robot [9]. Some particles live or down according to their comparative probability after an individually update phase, while the total particle number is static. The precision of the particle also depends on the particle density. The greater the number of particles in a specific area of the map, the higher will be the probability that the robot resides in the corresponding area of operation. By using the map, movement is computationally relaxed, concerning the simple arithmetical operations, allowing the use of a higher number of particles and accurate localization.

PF was first introduced in 1999, [10] in a localization context by the name of Monte Carlo Localization (MCL). In this situation, PF proposed a probabilistic method on how to evaluate the robot state in a prior defined map. This method is built on the hypothesis that the calculation of exterior values is associated with the robot's interior state such as the pose of the robot. After this, PF creates semi-random states in the world that provide an estimation on their corresponding state's probability to characterize the authentic state of the robot. The corresponding technique is required because the odometry (use of information from moving sensors to evaluate the change in location over time) of the robot deviates over time and may lose the accuracy highly. Therefore, by using the exterior sensors, this error can be corrected.

When the information is ambiguous and the environment grows in size, in such a situation the analytical calculations for the localization are going to fail. Because the sum of the probable causes to be measured becomes too large just after a limited round [11]. PFs signify the existing robot belief as a discrete probability distribution through the whole surrounding of operation or a position that is being measured i-e., the GPS individuated area. In the mid of every percept execution cycle, before deciding on the execution and after the perception, an update phase is taken. A new belief is erected which based on the existing belief phase, the percept from the sensors such as landmark sensing and the previous execution, resultantly the computational requirements don't rise over time.

A. CONTRIBUTIONS

The authors examined the localization reliability of KF, EKF, UKF, and PF in the above section. Nevertheless, the quality of such models under localization is not yet considered to the best of the author's knowledge. We proposed an EKF-based localization algorithm in our previous study and derived a numerical expression for the algorithm of localization. To this end, the authors use different algorithms to analyze the localization scheme in this work. Also, the authors derived the analytical expression for the localization of UKF and PF algorithms. The derived expressions are coherent in the sense that under different situations they can be used to evaluate the approaches of localization. In addition, for both motion and observation models, a covariance matrix is applied. Ultimately, UKF and PF algorithm tests of localization were analyzed and compared with different algorithms of localization. More specifically, in terms of cross-section area, length, time, velocity, etc., the proposed localization algorithms present decent accuracy while preserving reasonable computational intricacy.

B. ORGANIZATION

The rest of the paper is organized as follows. In the next section, the author presents the related work regarding localization algorithms. Section III presents the proposed localization algorithms and derives the numerical expressions for UKF and PF-based localization algorithms. The simulation results of each localization algorithm are explained in the subsections of section III. Section IV explains the comparison and analysis of the results. Finally, Section V presents the conclusions and provides prospects for future research work.

II. RELATED WORK

The KF-based localization has attracted significant consideration of the researchers over the last decades. A variety of solutions are presented regarding the KF-based localization algorithm, fast and prevailing development has been completed which is subsequent in several challenging solutions, counting both filtering and localization approach. Particular filtering approaches such as EKF and UKF-based estimates a state vector that consists of the robot observed landmark and existing pose. A detailed introduction to KF, EKF, UKF, and PF is discussed in the previous section. In the coming paragraphs, a detail about these localization algorithms and approaches is presented, and a comparison of the proposed algorithms is also presented.

UKF is a recursive state estimation approach basis on the unscented transform. It is a technique used to approximate a random variable's mean and covariance experiencing a non-linear conversion. Unlike the EKF, UKF applying a set of selected samples called sigma points for the representation of the state distribution, while EKF approximate the non-linear state equations and measurement models by applying the process of linearization. Several algorithms related to UKF are presented by the researchers such as in [12], a multi-sensor node fusion localization approach is presented utilizing the UKF in a rough environment. WSNs localization application is a crucial application in the indoor environment [13], [14]. In the non-line-of-sight (NLoS) atmosphere [15], the accuracy of localization is high, but the estimation may be contaminated by NLoS propagation, which resultantly decreases the localization accuracy. For this problem, the author presented the above approach to solving this problem which is a modified KF localization technique based on UKF.

A UKF-based filtering localization approaches for tracking and inertial navigation are presented in [16]–[19]. The approach is applied to discover the real-time location of moving targets in IoT surroundings. In this process, the information generated from the sensor nodes of IoT is involved to localize and track the moving targets. For this purpose, the least-square (LS) criterion-based mathematical model and square root UKF (SRUKF) based algorithm is applied to initialize the localization in the IoT environment. Next, a measurement method is applied to the inertial system by applying constraints of multiple view geometry. A version of the square root UKF (SRUKF) derived algorithm is proposed to incorporate the non-linear and complex structure. The state covariance root is propagated and updated in the SRUKF, thereby avoiding the breakdown of the state covariance. The technique is also applied in an NLoS environment that is based on the time-of-arrival (ToA) estimation. The sigma points of the unscented transformation are anticipated on the feasible area by solving the problem of constrained optimization. The feasible area is the intersection of various disks created by the NLoS estimation.

Furthermore, in [20]–[22], various approaches to the problem of simultaneous localization and mapping (SLAM) are presented. First, a sampling technique is proposed for the UKF which has the constant computational complexity resulting in the computational complexity of the UKF SLAM being established in the same order as that of the EKF SLAM. Second, an observability-constrained (OC)-UKF is suggested that guarantees the unobservable subspace of the UKF's linear-regression-based system is of the same size as the non-linear SLAM. Also, the limitations of the FastSLAM and Rao Blackwellized PF (RBPF) are investigated which are the derivation of the linear estimates of nonlinear functions and Jacobian matrices. Similarly, a real-time nonlinear method for SLAM is presented which is named as compressed UKF (CUKF). To address the problem of partial sampling, the author first proves the equivalence of the partial and full sampling approaches for the decoupled nonlinear schemes. Then a flattened arrangement is offered by reformulating the cross-correlation substances. However, RBFT and FastSLAM have two basic drawbacks. The first one is the derivation of the Jacobian matrices and the second one is the linear approximations of the non-linear functions. Therefore, calculation of the Jacobian is undesirable exertion, and imprecise approximation to the posterior covariance degenerates the filter reliability and estimate accuracy.

SLAM is an essential component in any autonomous mobile robot (AMR) or autonomous vehicle (AV). For this purpose, the authors in [23], [24] presented a SLAM-based localization algorithm to improve the performance of localization. A FastSLAM algorithm is proposed which consisted of an intelligent bat-inspired resampling whose iteration times can be adaptively tuned based on the filter diverging degree. Moreover, a square root cubature filter is merged into the algorithm for good proposal distribution and mapping results. An intelligent resampling phase is applied to FastSLAM, which is stimulated by microbat performances to attain the improved state of the robot. The projected resampling only functions on small-weight elements and thus decrease the computational load. In the proposed FastSLAM algorithm, the square root cubature Kalman filter (SRCKF) is merged for stepwise information of robot poses and map landscapes. The algorithms are compared based on two main aspects, the front-end is responsible for the extraction of important features from the sensor data as well as the data association. The second aspect, namely, the back-end is responsible for the probabilistic estimation purposes. The back-end is deeply reliant on the estimation concept and

almost the associated work uses one estimation algorithm or another. A SLAM robot tries to map an unidentified atmosphere while reckoning out where it is at. The complication comes from doing both these things at a similar time. The robot required to know its location before responding to the requirement of what the atmosphere looks like. The robot also has to count where it is without the advantage of previously taking a plan. SLAM, developed by Hugh Durrant-Whyte and John L. Leonard, is a way of solving this problem using specialized equipment and techniques. The procedure of resolving the problem initiates with the robot or unmanned vehicle (UV) itself. The type of robot utilized must have an exceptional odometry presentation. Odometry is the measure of how well the robot can estimate its own location. This is normally intended by the robot using the location of its wheels.

PF or sequential MCL are among the most widely used technique to offer a solution to the mobile robot localization problem. The PF solves the problem of localization as a Bayesian filtering problem to guesstimate the posterior or subsequent density of the state consuming weighted particles. It is a sequential Monte Carlo Bayesian (MCB) estimator which is probable to deliver additional valued evidence of the posterior. Specifically, when it has a multi-model shape or when the noise distributions are non-Gaussian.

In recent years, PF algorithms have solved numerous problems in the field of robot localization. The previous success of PF was only limited to low-dimensional measurement problems such as localization of robot in free defined maps [25]. The authors presented a variety of approaches that are mainly focused on the localization of robots in various environments such as in [26], [27], a self-localization technique is presented for a mobile robot that is based on the PF in active beacon system. The technique estimates the value of a mobile robot position and heading by applying the ultrasonic sensor and PF is applied to eliminate the measurement and process noise. The study [28], [29] presented an algorithm to solve the problem of SLAM in an unknown environment. An optimized RBPF algorithm is presented. The PF is extended to handle multi-robot SLAM problems. In this case, the initial or starting pose of the robot is known in which all the robots starting its motion from an identical place. Then an estimation is presented to solve the problem in which the robot initial pose is not known and the robot starts its motion from various positions. A Scale Invariant Feature Transform (SIFT) is proposed in [30] for robot localization that decreases the sum features generated by SIFT as well as their time of matching and extraction. Furthermore, a world and robot coordinate system are defined [31] which is based on the coordinate. The paper defined the state variable, state, and observation equations for the dynamic system. Besides, the paper also defines how to estimate the robot pose observation information by using the camera recognition information. By taking the real scene of Robocup, it defines UKF which is put into the PF framework to get Unscented PF (UPF) and then it is applied to understand self-localization. Finally, the localization technique is applied to the Nao robot by a sequence of simulation trials.

The problem of target localization and tracking has been intensively addressed by the researchers regarding WSNs [32]–[34]. These models present a PF technique to solve radio source localization by applying the measurements of only received signal strength indicator (RSSI), [35]. These models also take into account the antennae geometry, RF propagation, and ground reflection are presented. The model exploits the performance of free space wireless signals and gets the location estimates from the signal strength. The noisy location estimates are further used in a PF which estimates the posterior distribution of the location of the radio source. This technique is applicable with one or more targets and the error stabilizes to below 200 meters by applying 100 readings. Furthermore, in [36], the author presented a sound source localization and tracking technique by using an array of the microphone. The technique is based on the implementation of the frequency domain of a guided beam-former along with a PF tracking procedure. The PF is applied as a tracking framework that integrates a planned irregular source dynamic model for the recursive talker location estimation. But the main challenges in the regular variation of communicator locations which needs the process to capture the active communicator quickly. Also, the presence of noise in the background, reverberation, and interference presence degrades the performance of tracking. The above-mentioned algorithms presented well in their domain, but still, an improved version of localization is required to present better accuracy as compared to the previous algorithm. Therefore, in this paper, the author presented an advance localization algorithm that achieves a good level of accuracy in various circumstances.

III. PROPOSED LOCALIZATION ALGORITHMS

In this section, the authors present a detail of the proposed localization algorithms. To enhance the localization and tracking, the UKF and PF-based localization algorithms are involved. The proposed UKF and PF localization algorithms are analyzed and evaluated in different scenarios. Table 1 describes the notations used in this work.

A. LOCALIZATION THROUGH UNSCENTED KALMAN FILTER

The consistency of the UKF-based localization algorithm has received imperfect consideration by the researchers in the literature. The consistency of UKF is empirically inspected in [37]–[39], but no theoretical examination is available up to date, to the best of our knowledge. Therefore, in this article, the researcher expanded this study to the case of UKF-based localization. The authors presented the statistical linearization performance by using UKF. Additionally, the localization accuracy and coverage are analyzed, which achieves improved presentation than the previous localization algorithms. In addition, EKF-based updates are more vulnerable than UKF to large linearization errors. As mentioned in [40], a hybrid EKF and UKF algorithm, in which EKF is used as in the update state, while UKF for the computing the robot pose estimates and its covariance. While the presented algorithm

TABLE 1. Index of notation.

Notation	Description
x	State
$\acute{x}$	Mean of the state variable
X_{est}	Estimation state
X_{true}	True state
X_k	Current state
X_{k-1}	Previous state
x^a_{k-1}	Sigma point mean
P_{k-1}	Sigma point covariance
z_k	Measurement model
v_k	Process noise
n_k	Measurement noise
Q	Covariance matrix for prediction
R	Covariance matrix for observation
X_0	Sigma point
X_i	Sigma point at $i = 1, 2, 3, ..., n$
f	Function to calculate the predicted state
h	Function to calculate the predicted measurement
w	Importance weight
w^i_k	ith importance weight of the particle
x^i_k	ith state of the particle
$\sum_{i=0}^{2n} w^i$	Sum of all weights
n	Dimension of x
$\lambda = \alpha^2(n+k) - n$	Scaling parameter
α	Find the spreading of sigma point and mean
k	Secondary scaling parameter
R_k	Covariance matrix
K_k	Kalman gain
$X_{i,k\|k-1}$	Sigma point prediction
$Y_{i,k\|k-1}$	Improved sigma points
F, B	Transition state matrix
H	Output measurement matrix
V	Velocity m/sec
T	Operation time
t	Ending time of the operation
η	Constant of proportionality
$p(z_k \mid x^i_k)$	Importance factor
$p(x_k \mid z_{1:k})$	Posterior approximation
$f_k(x_k)$	Positive function for the state space
$f_0(x_0)$	Sample at initial guess
N	Number of samples
T_s	Robot sampling time
u	Vector of process model input
$\delta(.)$	Dirac delta function

achieves computational complication linearly through propagation and quadratic through the update state. Therefore, it is not possible to guarantee a positive description of the state covariance matrix during propagation.

EKF is the standard technique for the information integration and estimation of parameters, but EKF still exists some drawbacks. Using EKF, a non-linear system is linearized into a linear, in this case, the EKF accuracy can reach first order and also, EKF require to estimate the Jacobian matrix, which in some cases unable to estimate. Due to the above drawbacks and challenges, UKF has been used to present better performance as compared to the EKF algorithm and especially for the non-linear systems. UKF is based on unscented transformation, the approach used to estimate the statistics of the random variable. In UKF, some points are used to catch the actual covariance and mean of the random variables. Therefore, at least the accuracy reaches second order using UKF for non-linear systems. Also, by applying UKF, it is not required to calculate the Jacobian matrices as we calculated for the EKF-based algorithm. Resultantly, the UKF-based algorithm is more convenient and accurate as compared to the EKF-based algorithm.

Suppose that a state equation at the initial stage is;

$$x_k = f(x_{k-1}) + w_{k-1} \tag{3}$$

where $W_{k-1} \sim N(0, Q_k)$ is the process noise and f is the non-linear function as mentioned in the previous section. The x_k and x_{k-1} are existing and previous states at time t_k and t_{k-1}, respectively. Let suppose, a state variable x and covariance p is propagating through the non-linear equation.

$$x_k = f(x_{k-1}) + v_{k-1} \tag{4}$$

The mean for the state variable is $\acute{x}$ and the measurement equation is:

$$y_k = h(x_k) + n_k \tag{5}$$

where v_k is the process and n_k represents the measurement noise with the corresponding covariance matrix Q for prediction and covariance R for observation.

By calculating the sigma points, update time, and measurement update, the estimates of X_k can be found. A collection of deterministic test points with associated weights at the time $k-1$ is used to measure the sigma points.

$$X_{0,k-1} = \acute{x}_{k-1} \tag{6}$$

where X_0 is the sigma point at

$$X_{est} = \begin{bmatrix} 0 & 0 & 0 & 0 \end{bmatrix}^T \tag{7}$$

where X_{est} represents the estimated state and it will be the true state in the case if $X_{tru} = X_{est}$. To create the related weights for the sigma points:

$$X_{i,k-1} = \acute{x}_{k-1} + \left[\sqrt{(n+\lambda) \times P_{k-1}}\right]_i \tag{8}$$

where X_i represent the sigma points at $i = 1, 2, 3, \ldots, n$ and

$$X_{i,k-1} = \acute{x}_{k-1} - \left[\sqrt{(n+\lambda) \times P_{k-1}}\right]_{i-n} \tag{9}$$

where $i = n+1, n+2, \ldots, 2n$.

Generally, the weights are represented as:

$$w^m = \left[\frac{\lambda}{n+\lambda}\right] \tag{10}$$

and

$$w^c = \left[(\frac{\lambda}{n+\lambda}) + (1 - \alpha^2 + \beta)\right] \tag{11}$$

Now at time $t = 0$, the weights w^m and w^c will become:

$$w^m_0 = \left[\frac{\lambda}{n+\lambda}\right] \tag{12}$$

$$w^c_0 = \frac{\lambda}{(n+\lambda) + (1 - \alpha^2 + \beta)} \tag{13}$$

$$w^m_i = w^c_i = \frac{1}{2(n+\lambda)} \tag{14}$$

where $i = 1, 2, 3, \ldots, 2n$, n represent the dimension of x, $\lambda = \alpha^2(n + k) - n$ denote the scaling parameter, α find the spreading of sigma points around the mean of the state variable $\acute{x}$, and k denote the secondary scaling parameter (SSP).

Now to calculate the sigma points prediction with motion and observation model, the predicted mean and covariance is:

$$X_{i,k|k-1} = f(X_{i,k-1}) \tag{15}$$

$$\acute{\bar{x}} = \sum_{i=0}^{2n} w_i^m X_{i,k|k-1} \tag{16}$$

$$\acute{P}_k = \sum_{i=0}^{2n} w_i^c \left[X_{i,k|k-1} - \acute{\bar{x}}_k\right]\left[X_{i,k|k-1} - \acute{\bar{x}}_k\right]^T + Q_k \tag{17}$$

$$\dot{X}_{i,k|k-1} = \left[X_{0:2n,k|k-1} \;\; X_{0,k|k-1} + v\sqrt{Q_k} \;\; X_{0,k|k-1} - v\sqrt{Q_k}\right]_i \tag{18}$$

The sigma points were improved with additional points obtained from the process noise covariance matrix square root.

and

$$\dot{Y}_{i,k|k-1} = h(\dot{X}_{i,k|k-1}) \tag{19}$$

$$\acute{\bar{y}} = \sum_{i=0}^{2n^a} \dot{w}_i^m \dot{Y}_{i,k|k-1} \tag{20}$$

$$P_{yy,k} = \sum_{i=0}^{2n^a} \dot{w}_i^c \left[\dot{Y}_{i,k|k-1} - \acute{\bar{y}}_k\right]\left[\dot{Y}_{i,k|k-1} - \acute{\bar{y}}_k\right]^T + R_k \tag{21}$$

$$P_{xy,k} = \sum_{i=0}^{2n^a} \dot{w}_i^c \left[\dot{X}_{i,k|k-1} - \acute{\bar{x}}_k\right]\left[\dot{Y}_{i,k|k-1} - \acute{\bar{y}}_k\right]^T \tag{22}$$

In the above equations R_k represent the covariance matrix, $n^a = 2n$, and $v = \sqrt{n + \lambda}$ as can be seen in equation (10).

After calculating the sigma points and time updates, the measurement update and measurement noise are calculated. To update the covariance and state, Kalman gain is calculated.

$$K_k = P_{xy,k} \times \acute{P}^1_{yy,k} \tag{23}$$

$$\bar{X}_k = \acute{\bar{X}}_k + K_k(y_k - \acute{\bar{y}}_k) \tag{24}$$

$$P_k = \acute{P}_k - K_k \times P_{yy,k} \times K_k^T \tag{25}$$

Equation (23)-(25), represents a summary of the algorithm based on UKF. By giving the primary state:

$\acute{x}_0 = E[x_0]$ and $P_0 = E\left[(x_0 - \acute{x}_0) \times (x_0 - \acute{x}_0)^T\right]$.

$$R = \begin{bmatrix} cos(\theta) & sin(\theta) \\ -sin(\theta) & cos(\theta) \end{bmatrix} \tag{26}$$

where R is the covariance matrix of the measurement noise and the formula of the state can be represented as:

$$x_{k+1} = Fx_k + Bv_k \tag{27}$$

where F and B is

$$F = \begin{bmatrix} 1 & 0 & 0 & 0 \\ 0 & 1 & 0 & 0 \\ 0 & 0 & 1 & 0 \\ 0 & 0 & 0 & 0 \end{bmatrix} \tag{28}$$

$$B = \begin{bmatrix} dt \times cos(x(3)) & 0 \\ dt \times sin(x(3)) & 0 \\ 0 & dt \\ 1 & 0 \end{bmatrix} \tag{29}$$

$$H = \begin{bmatrix} 1 & 0 & 0 & 0 \\ 0 & 1 & 0 & 0 \\ 0 & 0 & 1 & 0 \\ 0 & 0 & 0 & 1 \end{bmatrix} \tag{30}$$

where F and B represents the transition state matrices. H is the output measurement matrix of the observation model.

1) SIMULATION RESULTS AND DISCUSSION

A simulation to evaluate the performance of the proposed UKF-based localization algorithm is performed in this section. In this simulation, in the first case, a time range is considered from 0 to 60 sec in which the initial time is $t = 0$ sec and the end time is $t = 60$ sec. The global time is $dt = 0.1$ sec. At first phase, the estimated state vector is set to be $X_{est} = \begin{bmatrix}0 & 0 & 0 & 0\end{bmatrix}^T$, in which $X_{true} = X_{est}$. The observation vector is set to be $z = \begin{bmatrix}0 & 0 & 0 & 0\end{bmatrix}^T$. After calculating the covariance matrix for prediction and observation, the sigma points are calculated as shown in equation (15)-(22). The UKF parameters are set to be in such way $\alpha = 0.001$, $\beta = 2$ and $\kappa = 0$. The size of the state vector is $n = length(X_{est})$. Then the weights w^m and w^c are calculated as can be seen in equations (10)-(14). The measurement noise R is calculated and then the sigma points prediction with the motion and observation model is calculated. The time for the input parameter calculation is $T = 10$ sec and the velocity is set to be $v = 1.0$ m/s which represents the linear speed of the robot. The factual data which is observed during the ground truth, the process noise is added and by applying Dead reckoning the current location is calculated which is the displacement of the previous location as can be seen in Fig. 6 (a-f).

In Fig. 1 (a-f), the velocity v and time t is kept constant throughout various iterations. In the second phase, the velocity is increased as before it was $v = 1.0$ m/s, but now we have increased to $v = 2.0$ m/s, $v = 3.0$ m/s, $v = 4.0$ m/s, $v = 5.0$ m/s, $v = 6.0$ m/s, and $v = 7.0$ m/s. In response to increasing the velocity, the coverage area of localization is also increased. In the UKF-based localization algorithm, the localization coverage is higher than the EKF-based localization as can be seen in Fig. 2 (a-f). Furthermore, the localization also varies with time. In Fig. 1 (a-f), we set the time $T = 10$ sec and then the time is upgraded to check the effectiveness of UKF-based localization. The time is varied to $T = 30$ sec and $T = 90$ sec. So, in this case, by increasing the time t, the localization accuracy is degrading and also the localization coverage area as shown

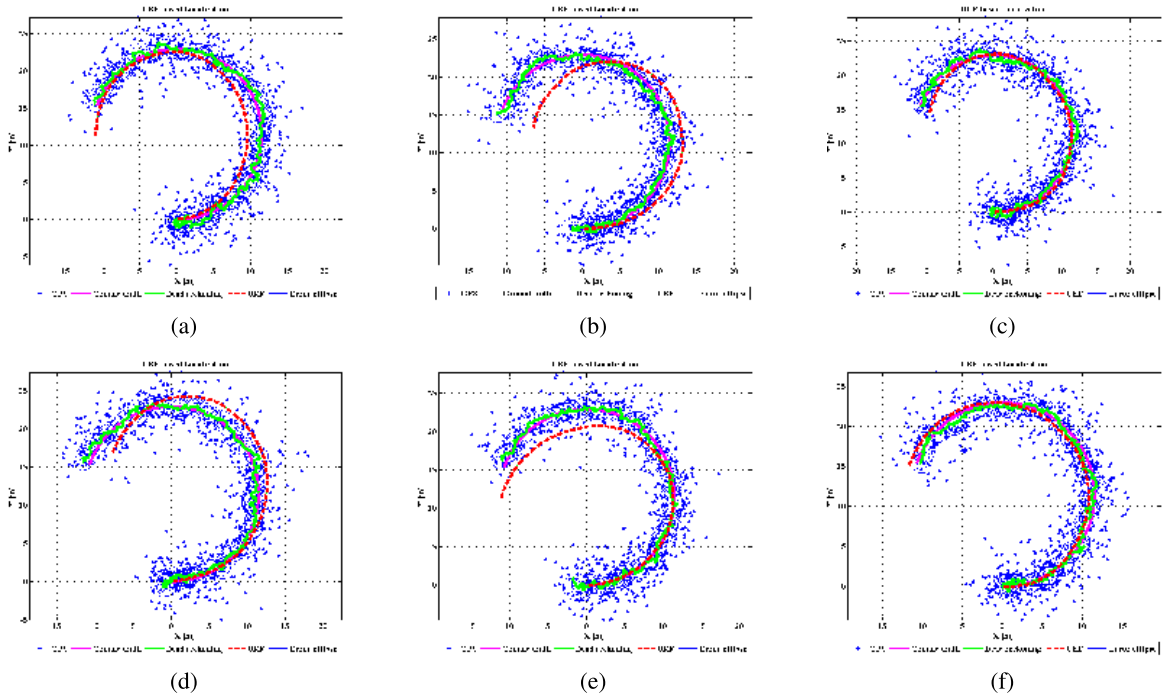

FIGURE 1. Comparison of various iterations for Localization based on the Unscented Kalman Filter (UKF) algorithm. In this case, the velocity is constant for all six iterations which is $v = 1.0$ m/s. The blue asterisks represent the GPS signals at various localizations, the pink line represents the ground truth which is required for the real-time localization. The green line represents the Dead reckoning to estimate the current position which is the displacement effect function used for the preceding position, the dashed red line represents the UKF localization, and the blue line is the error ellipse during the process of localization.

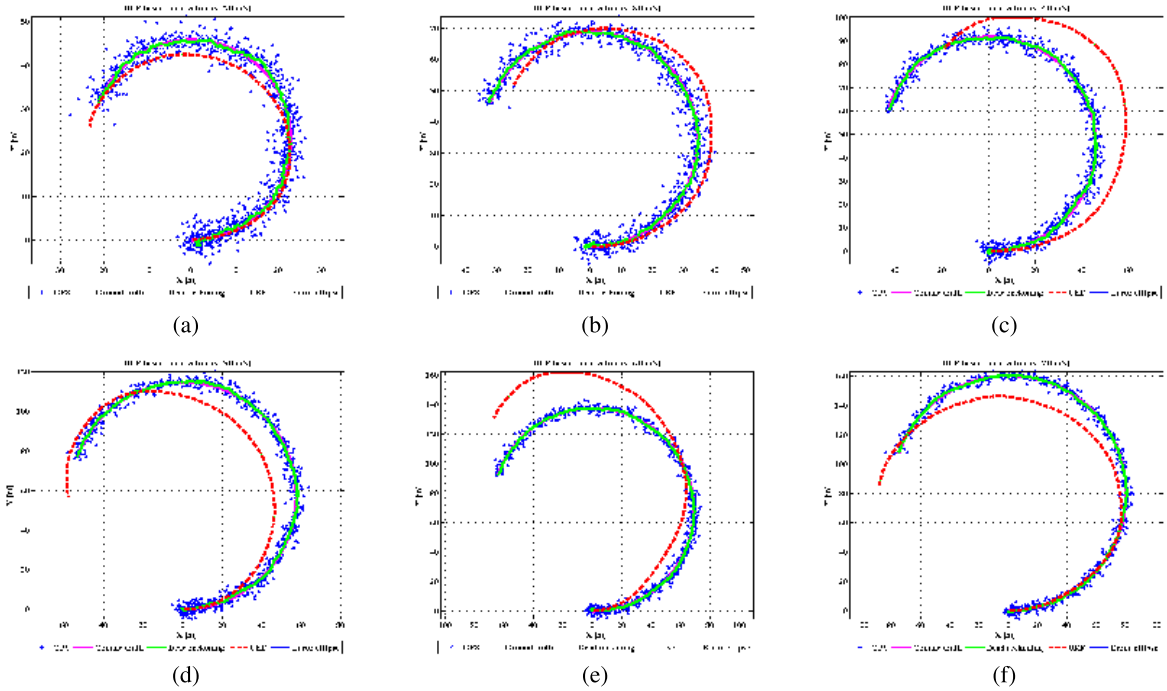

FIGURE 2. Localization based on Unscented Kalman Filter (UKF) with velocities ($v = 2.0$ m/s, $v = 3.0$ m/s, $v = 4.0$ m/s, $v = 5.0$ m/s).

in Fig. 3 (a-b). On the other side, by varying the end time the localization coverage and accuracy also effected. At the time $t = 30$ sec, the localization coverage area is decreased and at time $t = 90$ sec, there is no effect on the localization accuracy, however, the localization coverage is increased as shown in Fig. 4 (a-b).

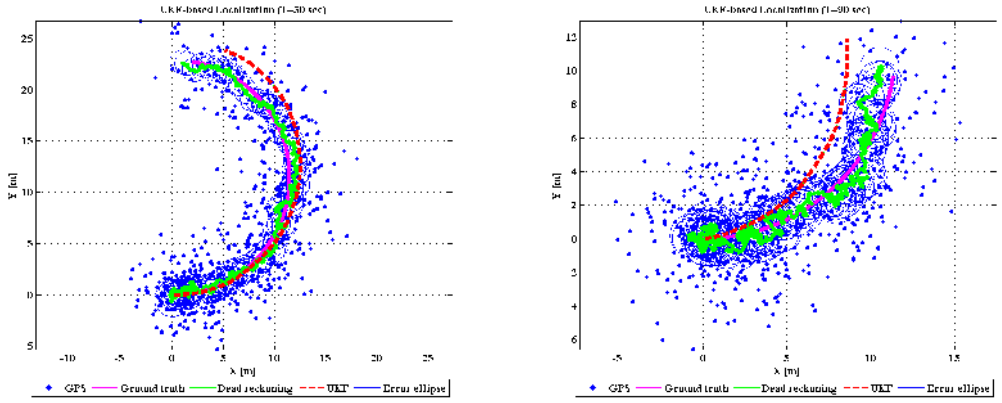

(a) (b)

FIGURE 3. Localization based on Unscented Kalman Filter (UKF) with time ($T = 30$ sec, $T = 90$ sec).

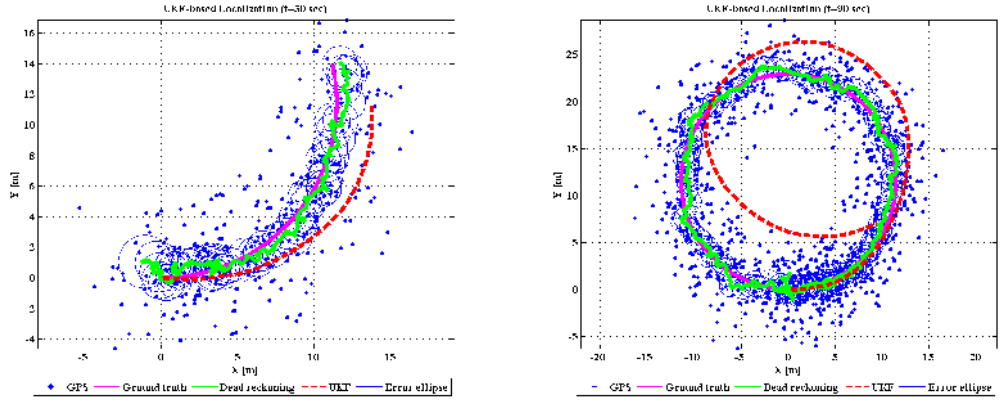

(a) (b)

FIGURE 4. Localization based on Unscented Kalman Filter (UKF) with the end-time ($t = 30$ sec, $t = 90$ sec).

B. LOCALIZATION THROUGH PARTICLE FILTER

In this section, the author presents a detail of the proposed PF localization algorithm. To improve the PF algorithm, PF is elaborate to retrieve the motion reservations animatedly by modifying the matrix of covariance. Furthermore, the robot can obtain a range of data or information from the radio-frequency identification (RFID) that its location is already prior known. For industrial requirements, the grid navigation spaces located with RFID tags are promising. Because each tag is capable of carrying 2D or 3D local environment data. Nonetheless, this technique requires a higher level of accuracy in the position of vehicles, otherwise, it may lead to collisions in the case of errors. In this regard, the author presented in [41], [42] an extended filtering method for finite impulse response (EFIR) that meets this requirement. This filter needs an optimal averaging interval but does not include the noise statistics which are mostly unknown in engineering. Also, when the robot starts its motion during localization, the sensor particle communicates with the robots. For regular PF, a vector x_k defines the position of a robot such as:

$$x_k = \begin{bmatrix} x_k & y_k \end{bmatrix}^T \tag{31}$$

For the first case, the authors consider the state estimation vector as $x_{est} = \begin{bmatrix} 0 & 0 & 0 \end{bmatrix}^T$ which offer an estimate $\bar{x}_k$ of the state x_k. Therefore, the prediction and measurement models are presented as:

$$x_k = f(x_{k-1}, w_k) \tag{32}$$

$$z_k = h(x_k, v_k) \tag{33}$$

where x_k and x_{k-1} are the current and previous states at time t_k and t_{k-1}. Similarly, f denote the transition of the state x_{k-1} and h denote the measurement function, respectively. In addition, w_k and v_k represent the discrete white zero-mean noise. To represent the covariance matrices Q and R, respectively, here $W_k \sim N(0, Q)$ i.e., $Q = diag(\sigma_x^2, \sigma_y^2)$ and $V_k \sim N(0, R)$ i.e., $R = diag(\sigma_{r,1}^2, \sigma_{r,2}^2, \ldots, \sigma_{r,n}^2)$. For the first case, the value of σ in the covariance matrix for prediction Q is set to be 0.1 and for the covariance matrix for observation is set to be 1. Let suppose, at time instant k, a set of particles can be expressed as:

$$S_k = [(x_k^i, w_k^i) \mid i = 1, 2, 3, \ldots, N_s] \tag{34}$$

$$w_k^i = \frac{p(x_k^i \mid z^k, u^k)}{p(x_k^i \mid u_k, x_{k-1}) p(x_{k-1} \mid z^{k-1}, u^{t-1})} \tag{35}$$

$$w_k^i = \frac{\eta p(z^k \mid x_k^i) p(x_k^i \mid u_k, x_{k-1}) p(x_{k-1} \mid z^{k-1}, u^{k-1})}{p(x_k^i \mid u_k, x_{k-1}) p(x_{k-1} \mid z^{k-1}, u^{k-1})} \tag{36}$$

$$w_k^i = \eta p(z_k \mid x_k^i) \tag{37}$$

In equation (33), the numerator represents the distribution of the target and denominator represents the proposal of the distribution. Where η is the constant and $p(z_k \mid x_k^i)$ is the importance factor.

Furthermore, let $f_k(x_k)$ is considered as a positive function for the state space. The algorithm of PF produce the samples from $f_k(x_k)p(x_k \mid z^k, u^k)$ in which at initial guess the samples are at $f_0(x_0)$. Next, to estimate the new samples, a random particle x_{k-1}^i is derived from X_{k-1} and the particle is distributed for N in accordant with $f_{k-1}(x_{k-1})p(x_{k-1} \mid z^{k-1}, u^{k-1})$. For the state $x_k^i \sim p(x_k \mid u_k, x_{k-1}^i)$, the importance weights can be calculated by using the function $f_k(x_k)$.

$$w_k^i = \frac{f_k(x_k^i)p(x_k^i \mid z^k, u^k)}{f_{k-1}(x_{k-1}^i)p(x_k^i \mid u_k, x_{k-1})p(x_{k-1} \mid z^{k-1}, u^{t-1})} \tag{38}$$

$$w_k^i = \frac{f_k(x_k^i)\eta p(z^k \mid x_k^i)p(x_k^i \mid u_k, x_{k-1})p(x_{k-1} \mid z^{k-1}, u^{k-1})}{f_{k-1}(x_{k-1}^i)p(x_k^i \mid u_k, x_{k-1})p(x_{k-1} \mid z^{k-1}, u^{k-1})} \tag{39}$$

By replacing the constant of proportionality, equation (37) will become:

$$w_k^i \propto p(z_k \mid x_k^i) \times \frac{f_k(x_k^i)}{f_{k-1}(x_{k-1}^i)} \tag{40}$$

The motion of the particle can be predicted by using the particle which contains the location of the robot at time instant k:

$$x_k^i = f(x_{k-1}^i) + w_k \tag{41}$$

$$x_k^i = x_{k-1}^i + \begin{bmatrix} v_k \times T_s \times cos\theta_k \\ v_k \times T_s \times sin\theta_k \end{bmatrix} + w_k \tag{42}$$

where T_s denote the robot sampling time. The state estimate $\bar{x}_{k|k-1}$ expectation can also be represented by:

$$\bar{x}_{k|k-1} = f(\bar{x}_{k-1|k-1}) \tag{43}$$

$$P_{k|k-1} = \sum_{i=1}^{N_s} w_k^i \times \left[x_k^i - \bar{x}_{k|k-1}\right] \times \left[x_k^i - \bar{x}_{k|k-1}\right]^T + Q \tag{44}$$

where x_k and x_{k-1} are the current and previous states at time t_k, t_{k-1}. Q is the covariance matrix and w is the importance weights. The subsequent approximation $p(x_k \mid z_{1:k})$ and the state estimation $\bar{x}_{k|k}$ can be approximated by [43]:

$$p(x_k \mid z_{1:k}) \approx \sum_{i=1}^{N_s} w_k^i \times \delta(x_k - x_k^i) \tag{45}$$

$$\bar{x}_{k|k} = E[x_k \mid z_{1:k}] \tag{46}$$

$$\bar{x}_{k|k} = \int x_k \times p(x_k \mid z_{1:k})dx_k \approx \sum_{i=1}^{N_s} w_k^i \times x_k^i \tag{47}$$

$$P_{k|k} = \sum_{i=1}^{N_s} w_k^i \times \left[x_k^i - \bar{x}_{k|k}\right] \times \left[x_k^i - \bar{x}_{k|k}\right]^T \tag{48}$$

where $\delta(\ldots)$ represent the Dirac delta function. The above posterior approximation is considered as a posterior belief function and approximated by a set of N samples as can be seen in [44], [45].

$$F = \begin{bmatrix} 1 & 0 & 0 \\ 0 & 1 & 0 \\ 0 & 0 & 1 \end{bmatrix} \tag{49}$$

$$B = \begin{bmatrix} dt \times cos(x(3)) & 0 \\ dt \times sin(x(3)) & 0 \\ 0 & dt \end{bmatrix} \tag{50}$$

Similarly, in equation (28) and (29), here F and B represents the transition state matrices of the motion model.

1) SIMULATION RESULTS AND DISCUSSION

In this section, a simulation is performed to evaluate the performance of the proposed PF-based localization algorithm. For the PF-based localization algorithm, the value of the parameter is almost similar to the UKF-based localization algorithm but some parameters are varying from UKF and therefore, the performance of PF also varying from the UKF. At the initial phase, the time range is considered as $t = 60$ sec and the global time is $dt = 0.1$ sec. The estimated state vector is set to be $Xest = \begin{bmatrix}0 & 0 & 0\end{bmatrix}^T$ in which the true state is $x_{True} = x_{Est}$. After calculating the covariance matrix for prediction and observation, the sigma points are calculated. The importance weights w_i are calculated by using the function $f_k(x_k)$ as shown in equations (35)-(40). The effective sample size is $N_{eff} = 1.0$ and if this is left empty, the number of components in the pdf will be taken as N_{eff}. However, if we have pre-clustered the data, then we must set the N_{eff} to the number of original samples in clustering. The transition state matrices F and B of the motion model are calculated in equations (49) and (50). At the initial phase, the time is set to be $T = 10$ sec and the velocity is set to be $v = 1.0$ m/s, which is the robot linear speed during the localization process. When the robot starts it's motion from $t = 0$ sec, during it's traveling the sensor particles communicate with the robot while performing localization. The process noise is added and by applying Dead reckoning the current location is calculated which is the displacement of the previous location. In this phase ($v = 1.0$ m/s), during the six iterations, the coverage and localization time is ranging from 4.598 sec to 5.0987 sec as shown in Fig. 5 (a-f) and results in Table 2.

During the first phase, the time and velocity for all iterations were constant see Fig. 5 (a-f). In the second phase, the velocity is decreased from $v = 1.0$ m/s to $v = 0.1$ m/s, $v = 0.2$ m/s, $v = 0.3$ m/s, $v = 0.4$ m/s, $v = 0.5$ m/s, and $v = 0.6$ m/s. By reducing the velocities, the localization time is almost similar to the first phase, but the coverage area is reduced highly as can be seen in Fig. 6 (a-f). Alternatively, by increasing the time from $T = 10$ sec to $T = 30$ sec and $T = 90$ sec, the time consumption is constant but the coverage area is reducing as shown in Fig. 7 (a-b). Furthermore, in the case of decreasing the end time t of localization from $t = 60$ sec to $t = 30$ sec, the coverage area and localization time also decrease which is $t = 2.4412$ sec. It represents that if the time is maximum, the coverage area

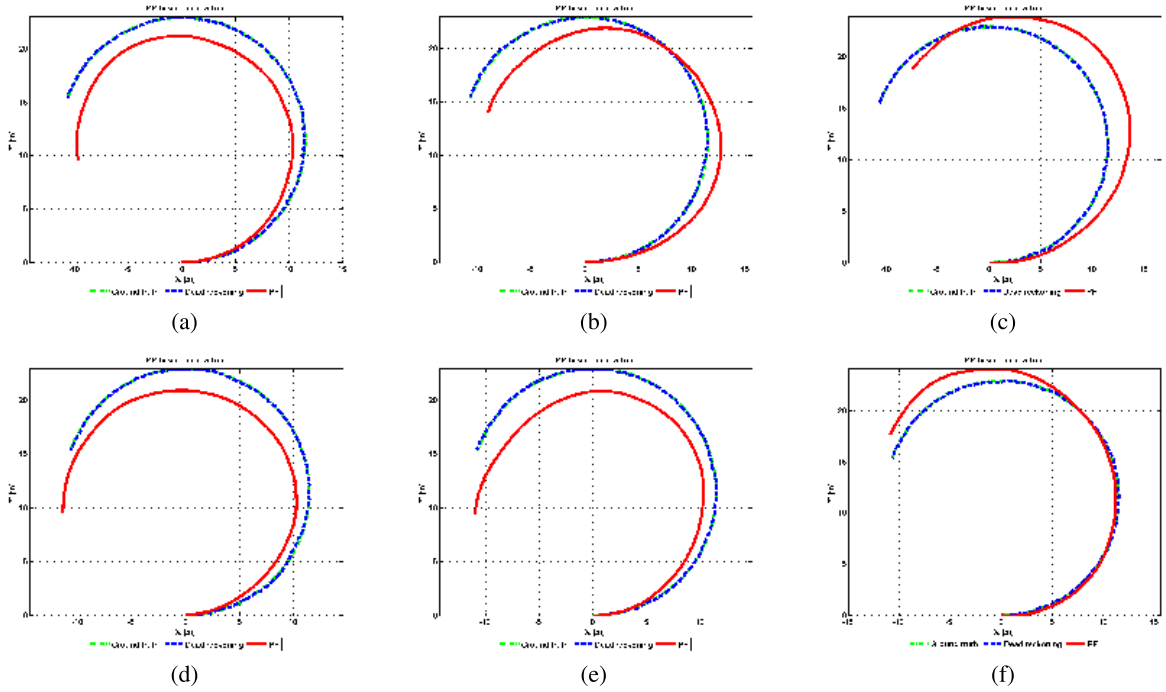

FIGURE 5. Comparison of various iterations for Localization based on the Particle Filter (PF) algorithm. In this case, the velocity is constant for all six iterations which is $v = 1.0$ m/s. The green dashed line represents the ground truth which is required for the real-time localization, the blue dashed line is the Dead reckoning to estimate the current position which is the displacement effect function used for the preceding position, and the red line represents the PF localization.

TABLE 2. Simulations parameters.

Parameters used	Assigned values
Initial time (t)	0 sec
End time (t)	60 sec
Global time (t)	0.1 sec
Input time (T)	10 sec
Initial velocity (v)	1.0 m/s
Yaw rate	5 deg/sec
Degree to radian	180°
Radian to degree	180°
UKF updated velocities	2.0 m/s-7.0 m/s
UKF updated time for input parameters (T)	30-60 sec
Sigma points (i)	i=1,2,3,...,n
UKF Parameter (α)	0.001
UKF Parameter (β)	2
UKF Parameter (κ)	0
Covariance matrix for prediction (Q)	0.1
Covariance matrix for observation (Q)	1
Weights (w_i)	i=1,2,3,...,2n
PF updated velocities (v)	0.1 m/s-0.6 m/s
N_{eff}	1.0
Updated end time (t)	90 sec
Total range	360°

and localization will be more efficient and it may consume more time as compared to the previous case. Therefore, by increasing the end time t of localization from $t = 60$ sec to $t = 90$ sec, the localization time is increased but resultantly gives high coverage which covers a total 360° area as shown in Fig. 8 (a-b).

IV. COMPARISON AND RESULTS ANALYSIS

In the previous sections, the simulation results are widely detailed for well understanding of the readers. In this section, we will discuss more the results and comparison of these results with each-others and previous algorithms used for the purpose of localization in various research articles. Our proposed localization algorithms work as a platform for the other localization algorithms that are discussed in detail in the literature. Every algorithm works good in their domain and considers various aspects during the localization process but still exist some limitations, for example, some algorithms do not consider the prior data for the unknown parameters, etc.

In section 3, Fig. 1 (a-f) and Fig. 5 (a-f) represent the localization performance of UKF and PF-based localization algorithms, respectively. In the first phase of UKF and PF, the authors considered a constant velocity of $v = 1.0$ m/s and time $T = 10$ sec throughout the six iterations. For both algorithms, the authors considered six iterations in the first case, to evaluate the localization performance in a better way. In the second phase of UKF-based localization algorithm, the localization performance is evaluated while increasing the velocity from $v = 1.0$ m/s to $v = 2.0$ m/s, $v = 3.0$ m/s, $v = 4.0$ m/s, $v = 4.0$ m/s, $v = 5.0$ m/s, $v = 3.0$ m/s, and $v = 7.0$ m/s,. Resultantly, by increasing the velocity v, the coverage area is also increasing as can be seen in Fig. 2 (a-f). UKF-based localization algorithm presents a good level of accuracy as compared to the EKF-based algorithm Fig. 2 (a-f). While in the second phase of the PF-localization algorithm,

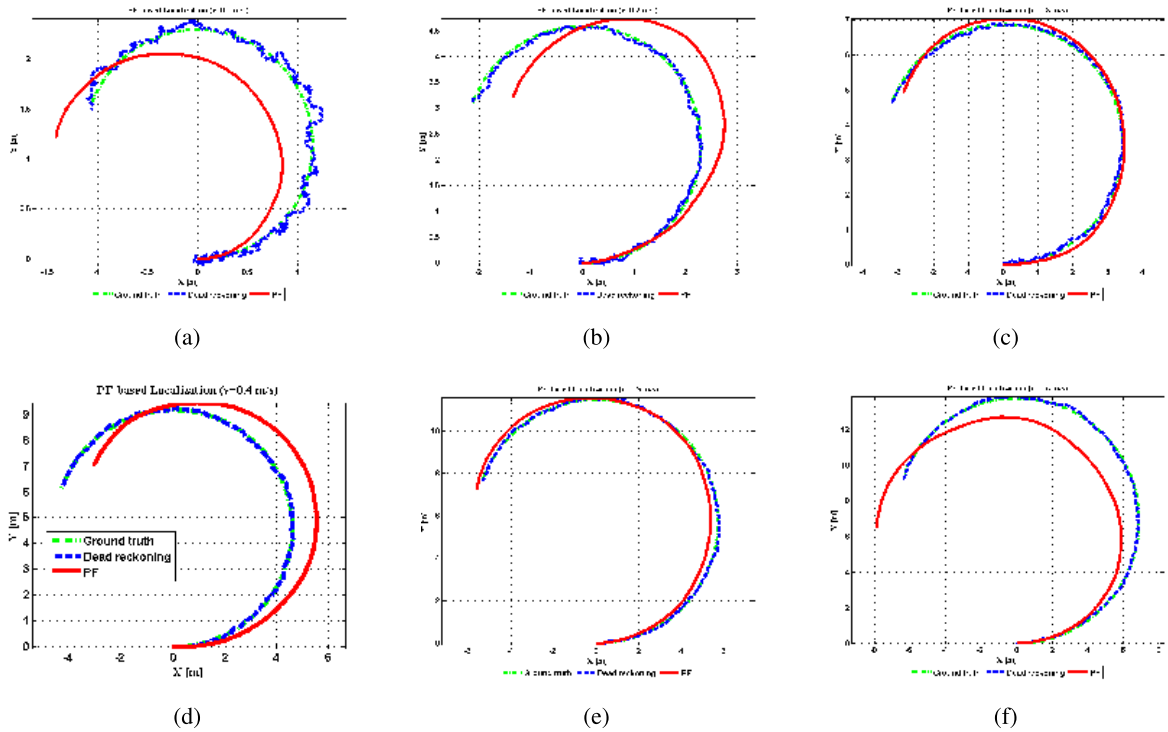

FIGURE 6. Localization based on Particle Filter (PF) with velocities ($v = 0.1$ m/s, $v = 0.2$ m/s, $v = 0.3$ m/s, $v = 0.4$ m/s, $v = 0.5$ m/s, $v = 0.6$ m/s).

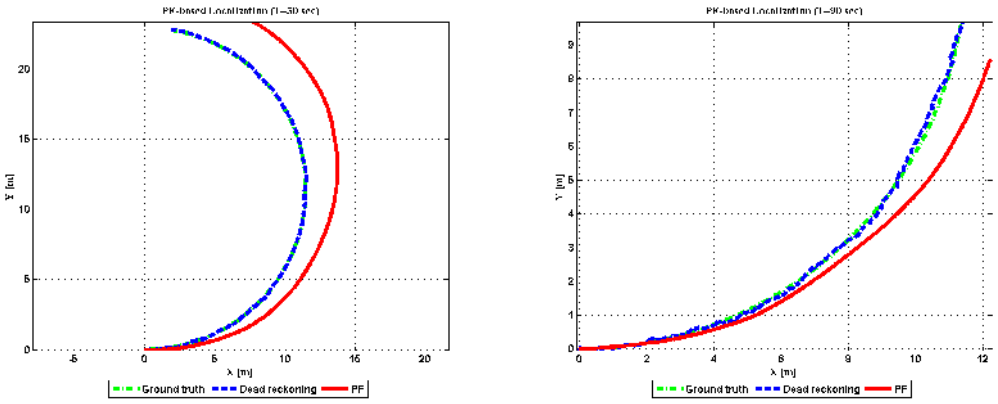

FIGURE 7. Localization based on Particle Filter (PF) with time ($T = 30$ sec, $T = 90$ sec).

the velocity is reduced from $v = 1.0$ m/s to $v = 0.1$ m/s, $v = 0.2$ m/s, $v = 0.3$ m/s, $v = 0.4$ m/s, $v = 0.5$ m/s, and $v = 0.6$ m/s and performed six iterations. Resultantly, to reduce the velocity v, the localization time is almost similar to the first case, but the coverage area is reduced highly as can be seen in Fig. 6 (a-f). The remaining detail about time variance is discussed in detail in the previous sections.

During the localization process, the time consumption and coverage time are evaluated as shown in Table 3. In our previous study, the authors presented an EKF-based localization algorithm and the results of EKF-based localization are compared with the UKF and PF in Table 3. Among all these three localization algorithms i.e EKF, UKF, and PF, the PF-based localization algorithm consumes less time as compared to EKF and UKF at $v = 1.0$ m/s. By doing further iterations, in between EKF and UKF localization algorithms, UKF is consuming less time and performing well as compare to the EKF localization algorithm. The proposed localization algorithms are highly sensitive to time t and velocity v as discussed above.

To compare the proposed localization algorithms with other localization algorithms, our localization algorithms

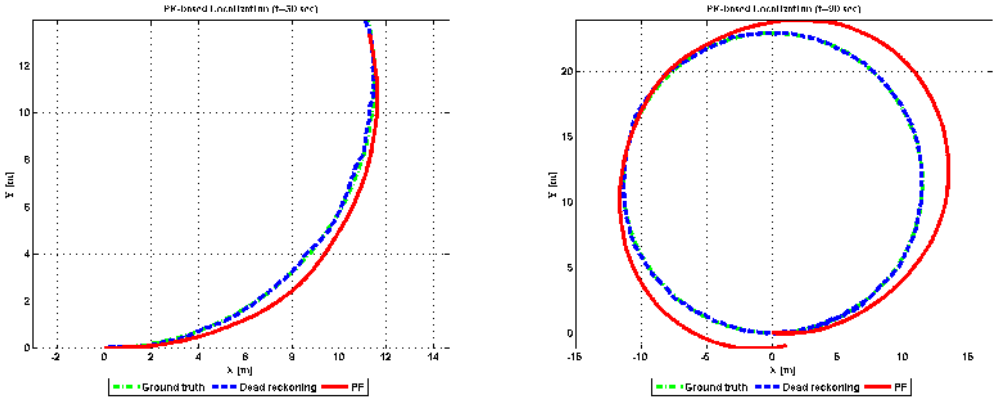

(a) (b)

FIGURE 8. Localization based on Particle Filter (PF) with end-time ($t = 30$ sec, $t = 90$ sec).

TABLE 3. Time consumption comparison of EKF, UKF, and PF during localization.

Velocities (V)	Iterations	$T_{EKF}(Sec)$	$T_{UKF}(Sec)$	$T_{PF}(Sec)$
"$V_1 = 1.0$ m/s"	One	6.8369	5.8049	5.6805
	Two	6.6364	5.8529	5.4942
	Three	6.8034	6.0852	5.6570
	Four	6.2625	5.8547	5.5314
	Five	6.7175	5.8959	5.3960
	Six	6.5195	6.1043	5.3561
"$V_2 = 2.0$ m/s"	One	5.9077	5.7425	-
"$V_3 = 3.0$ m/s"	One	6.4833	5.8621	-
"$V_4 = 4.0$ m/s"	One	6.6183	5.7759	-
"$V_5 = 5.0$ m/s"	One	6.3488	5.6934	-
"$V_6 = 6.0$ m/s"	One	6.4298	5.7417	-
"$V_7 = 7.0$ m/s"	One	6.2452	5.7542	-
"$V_8 = 8.0$ m/s"	One	6.4508	5.9540	-
"$V_9 = 9.0$ m/s"	One	6.5239	6.0276	-
"$V_{10} = 10.0$ m/s"	One	6.1087	5.8449	-

perform better regarding various aspects such as localization coverage and time. It is encouraged by the fact that the proposed algorithms can present a better estimate of time and velocity. The EKF and UKF are compared in [46] to evaluate the effectiveness of the two widely used filters for non-linear systems, in reconstructing the unknown environment where a mobile robot is moving. The reconstruction is obtained from the robot's onboard sonar sensors. In [47] the author proposed an improved UKF localization algorithm to reduce the impacts of packet loss during the process of localization. Rather than ignoring the missing measurements which are caused by the packet loss, the algorithm exploits the calculated measurement errors to estimate missing measurements. Moreover, a TDoA-based localization technique using the PF with multiple motions is presented in [48] for non-cooperative target tracking in 2D. For this purpose, three motion models, constant acceleration and velocity, two-channel models, LoS and NLoS, are considered to define the route of a mobile terminal in mixed LoS/NLoS situations. The particle filtering method is applied for state estimation from a set of nonlinear TDoA measurements, and the interacting various models are used to mix the various motions and channel models to improve the positioning accuracy. Various localization algorithms are proposed by the researchers [49]–[53], each algorithm performs well in its domain and presents their performance. Some algorithm focuses on the accuracy of localization, some focuses on the coverage of localization, time, energy consumption, etc. To the best of the authors knowledge, the proposed localization algorithms perform well as compared to the state-of-the-art localization algorithms in this area.

V. CONCLUSION

In this paper, the authors presented the performance of UKF and PF-based localization algorithms. As we mentioned in the previous sections about the EKF-based localization which was the part of our previous study. In this work, the authors presented a very detail about the localization of UKF and PF-based localization algorithms. Firstly, an analytical expression for the UKF-based algorithm is presented and evaluated their performance. Secondly, the PF-localization is presented and evaluated their performance. Each localization algorithm performs well in their domain. Several aspects regarding localization are considered in this study such as the velocity, time, distance, cross-section area, coverage, etc. The performance of the proposed localization algorithms is evaluated deeply by performing several iterations as shown in the figures. The proposed localization algorithms present good accuracy while maintaining reasonable computational intricacy. The proposed UKF and PF localization algorithms are compared with each other based on their performance and also with the EKF-based localization algorithm as shown in Table 3. Among all these three algorithms, the PF-based

localization algorithm presents a good level of performance while consuming very less time as compared to the EKF and UKF-based algorithms. The proposed localization algorithms can apply any type of localization system, particularly for the robot localization. The result shows an excellent localization quality within a limited time, given the harsh physical environment and several problems during localization. The results of the simulation show that the proposed localization algorithms can be used for different purposes such as target tracking, robot localization, and can improve localization performance. In the future, the authors will focus on the comparative analysis of the EKF, UKF, and PF localization algorithms. Besides this, the authors will try to improve the localization performance of the EKF, UKF, and PF-based localization algorithms.

REFERENCES

[1] P. Thulasiraman and K. A. White, "Topology control of tactical wireless sensor networks using energy efficient zone routing," *Digit. Commun. Netw.*, vol. 2, no. 1, pp. 1–14, Feb. 2016.

[2] N. A. S. Alwan and Z. M. Hussain, "Gradient descent localization in wireless sensor networks," in *Wireless Sensor Networks: Insights and Innovations*. Joondalup, WA, Australia: Edith Cowan Univ., 2017, p. 39.

[3] A. Pughat and V. Sharma, "Performance analysis of an improved dynamic power management model in wireless sensor node," *Digit. Commun. Netw.*, vol. 3, no. 1, pp. 19–29, Feb. 2017.

[4] A. Singh, S. Kumar, and O. Kaiwartya, "A hybrid localization algorithm for wireless sensor networks," *Procedia Comput. Sci.*, vol. 57, pp. 1432–1439, 2015.

[5] H. Zhang, Q. Huang, F. Li, and J. Zhu, "A network security situation prediction model based on wavelet neural network with optimized parameters," *Digit. Commun. Netw.*, vol. 2, no. 3, pp. 139–144, Aug. 2016.

[6] I. Ullah, Y. Liu, X. Su, and P. Kim, "Efficient and accurate target localization in underwater environment," *IEEE Access*, vol. 7, pp. 101415–101426, 2019.

[7] J. Yang, Z. Fei, and J. Shen, "Hole detection and shape-free representation and double landmarks based geographic routing in wireless sensor networks," *Digit. Commun. Netw.*, vol. 1, no. 1, pp. 75–83, Feb. 2015.

[8] G. A. Terejanu, "Unscented kalman filter tutorial," Univ. Buffalo, Buffalo, NY, USA, Tech. Rep., 2011.

[9] A.-C. Bellini, "4D-particle filter localization for a simulated UAV," in *Proc. PAI*, 2012, pp. 60–66.

[10] A. Heilig, I. Mamaev, B. Hein, and D. Malov, "Adaptive particle filter for localization problem in service robotics," in *Proc. MATEC Web Conf.*, vol. 161, 2018, p. 01004.

[11] L. Marchetti, G. Grisetti, and L. Iocchi, "A comparative analysis of particle filter based localization methods," in *Proc. Robot Soccer World Cup*, 2006, pp. 442–449.

[12] Y. Huang, Y. Jing, and Y. Shi, "Multi-sensor node fusion localization using unscented Kalman filter in rough environments," in *Proc. IEEE Chin. Control Decis. Conf. (CCDC)*, Jun. 2018, pp. 5476–5481.

[13] A. L. Sreenivasulu and P. C. Reddy, "NLDA non-linear regression model for preserving data privacy in wireless sensor networks," *Digit. Commun. Netw.*, to be published.

[14] X. Su, I. Ullah, X. Liu, and D. Choi, "A review of underwater localization techniques," *J. Sensors*, to be published.

[15] J. M. Huerta, J. Vidal, A. Giremus, and J.-Y. Tourneret, "Joint particle filter and UKF position tracking in severe non-line-of-sight situations," *IEEE J. Sel. Topics Signal Process.*, vol. 3, no. 5, pp. 874–888, Oct. 2009.

[16] R. Zhan and J. Wan, "Iterated unscented Kalman filter for passive target tracking," *IEEE Trans. Aerosp. Electron. Syst.*, vol. 43, no. 3, pp. 1155–1163, Jul. 2007.

[17] J. Guo, H. Zhang, Y. Sun, and R. Bie, "Square-root unscented Kalman filtering-based localization and tracking in the Internet of Things," *Pers. Ubiquit Comput.*, vol. 18, no. 4, pp. 987–996, Apr. 2014.

[18] Z. Xian, J. Lian, M. Shan, L. Zhang, X. He, and X. Hu, "A square root unscented Kalman filter for multiple view geometry based stereo cameras/inertial navigation," *Int. J. Adv. Robotic Syst.*, vol. 13, no. 5, Sep. 2016, Art. no. 172988141666485.

[19] S. Yousefi, X.-W. Chang, and B. Champagne, "Mobile localization in non-line-of-sight using constrained square-root unscented Kalman filter," *IEEE Trans. Veh. Technol..*, vol. 64, no. 5, pp. 2071–2083, May 2015.

[20] G. P. Huang, A. I. Mourikis, and S. I. Roumeliotis, "A quadratic-complexity observability-constrained unscented Kalman filter for SLAM," *IEEE Trans. Robot.*, vol. 29, no. 5, pp. 1226–1243, Oct. 2013.

[21] C. Kim, R. Sakthivel, and W. Chung, "Unscented FastSLAM: A robust and efficient solution to the SLAM problem," *IEEE Trans. Robot.*, vol. 24, no. 4, pp. 808–820, Aug. 2008.

[22] J. Cheng, J. Kim, Z. Jiang, and X. Yang, "Compressed unscented Kalman filter-based SLAM," in *Proc. IEEE Int. Conf. Robot. Biomimetics (ROBIO)*, Dec. 2014, pp. 1602–1607.

[23] M. Lin, C. Yang, D. Li, and G. Zhou, "Intelligent filter–based SLAM for mobile robots with improved localization performance," *IEEE Access*, vol. 7, pp. 113284–113297, 2019.

[24] M. Osman, A. Hussein, and A. Al-Kaff, "Intelligent vehicles localization approaches between estimation and information: A review," in *Proc. IEEE Int. Conf. Veh. Electron. Saf. (ICVES)*, Sep. 2019, pp. 1–8.

[25] S. Thrun, "Particle filters in robotics," in *Proc. 18th Conf. Uncertainty Artif. Intell.*, 2002, pp. 511–518.

[26] D. Fox, S. Thrun, W. Burgard, and F. Dellaert, "Particle filters for mobile robot localization," in *Proc. Sequential Monte Carlo Methods Pract.*, 2001, pp. 401–428.

[27] J. Woo, Y.-J. Kim, J.-O. Lee, and M.-T. Lim, "Localization of mobile robot using particle filter," in *Proc. SICE-ICASE Int. Joint Conf.*, Oct. 2006, pp. 3031–3034.

[28] A. Howard, "Multi-robot simultaneous localization and mapping using particle filters," *Int. J. Robot. Res.*, vol. 25, no. 12, pp. 1243–1256, Dec. 2006.

[29] C. Ji, H. Wang, and Q. Sun, "Improved particle filter algorithm for robot localization," in *Proc. 2nd Int. Conf. Educ. Technol. Comput.*, vol. 4, Jun. 2010, pp. V4–174.

[30] H. Tamimi, H. Andreasson, A. Treptow, T. Duckett, and A. Zell, "Localization of mobile robots with omnidirectional vision using particle filter and iterative SIFT," *Robot. Auto. Syst.*, vol. 54, no. 9, pp. 758–765, Sep. 2006.

[31] D. Li, Q. Chen, and Z. Zeng, "Self-localization algorithm of mobile robot based on unscented particle filter," in *Proc. 37th Chin. Control Conf. (CCC)*, Jul. 2018, pp. 5459–5464.

[32] N. Wagle and E. Frew, "A particle filter approach to WiFi target localization," in *Proc. AIAA Guid., Navigat., Control Conf.*, Aug. 2010, p. 7750.

[33] I. Ullah, J. Chen, X. Su, C. Esposito, and C. Choi, "Localization and detection of targets in underwater wireless sensor using distance and angle based algorithms," *IEEE Access*, vol. 7, pp. 45693–45704, 2019.

[34] P. Soriano, F. Caballero, and A. Ollero, "RF-based particle filter localization for wildlife tracking by using an UAV," in *Proc. 40th Int. Symp. Robot.*, Barcelona, Spain, Mar. 2009, pp. 239–244.

[35] S. A. Arif, M. H. Niaz, N. Shabbir, M. H. Zafar, S. R. Hassan, and A. Ur Rehman, "RSSI based trilatertion for outdoor localization in ZigBee based wireless sensor networks (WSNs)," in *Proc. 10th Int. Conf. Comput. Intell. Commun. Netw. (CICN)*, Aug. 2018, pp. 1–5.

[36] J.-M. Valin, F. Michaud, and J. Rouat, "Robust localization and tracking of simultaneous moving sound sources using beamforming and particle filtering," *Robot. Auto. Syst.*, vol. 55, no. 3, pp. 216–228, 2007.

[37] K. Wu, V. G. Reju, A. W. H. Khong, and S. T. Goh, "Swarm intelligence based particle filter for alternating talker localization and tracking using microphone arrays," *IEEE/ACM Trans. Audio Speech Lang. Process.*, vol. 25, no. 6, pp. 1384–1397, Jun. 2017.

[38] G. P. Huang, A. I. Mourikis, and S. I. Roumeliotis, "A quadratic–complexity observability–constrained unscented Kalman filter for SLAM," *IEEE Trans. Robot.*, vol. 29, no. 5, pp. 1226–1243, Oct. 2013.

[39] S. Yousefi, X.-W. Chang, and B. Champagne, "Mobile localization in non-line-of-sight using constrained square–root unscented Kalman filter," *IEEE Trans. Veh. Technol.*, vol. 64, no. 5, pp. 2071–2083, May 2015.

[40] Y. Huang, Y. Jing, and Y. Shi, "Multi-sensor node fusion localization using unscented kalman filter in rough environments," in *Proc. Chin. Control Decis. Conf. (CCDC)*, Jun. 2018.

[41] J. Andrade-Cetto, T. Vidal-Calleja, and A. Sanfeliu, "Unscented transformation of vehicle states in SLAM," in *Proc. IEEE Int. Conf. Robot. Autom.*, Jan. 2006, pp. 323–328.

[42] J. J. Pomarico-Franquiz and Y. S. Shmaliy, "Accurate self–localization in RFID tag information grids using FIR filtering," *IEEE Trans. Ind. Informat.*, vol. 10, no. 2, pp. 1317–1326, May 2014.
[43] J. J. Pomarico-Franquiz, M. Granados-Cruz, and Y. S. Shmaliy, "Self–localization over RFID tag grid excess channels using extended filtering techniques," *IEEE J. Sel. Topics Signal Process.*, vol. 9, no. 2, pp. 229–238, Mar. 2015.
[44] B.-F. Wu and C.-L. Jen, "Particle-filter-based radio localization for mobile robots in the environments with low–density WLAN APs," *IEEE Trans. Ind. Electron.*, vol. 61, no. 12, pp. 6860–6870, Dec. 2014.
[45] M. Di Rocco and G. Ulivi, "An efficient implementation of a particle filter for localization using compass data," *IFAC Proc. Vols.*, vol. 43, no. 16, pp. 217–222, 2010.
[46] L. D'Alfonso, A. Grano, P. Muraca, and P. Pugliese, "Extended and unscented Kalman filters in a cells-covering method for environment reconstruction," in *Proc. IEEE 15th Int. Conf. Control Autom. (ICCA)*, Jul. 2019, pp. 1557–1562.
[47] X. Bai, Z. Zhang, L. Liu, X. Zhai, J. Panneerselvam, and L. Ge, "Enhancing localization of mobile robots in distributed sensor environments for reliable proximity service applications," *IEEE Access*, vol. 7, pp. 28826–28834, 2019.
[48] N. Xia and M. A. Weitnauer, "TDOA–based mobile localization using particle filter with multiple motion and channel models," *IEEE Access*, vol. 7, pp. 21057–21066, 2019.
[49] J. Poterjoy, "A localized particle filter for high–dimensional nonlinear systems," *Monthly Weather Rev.*, vol. 144, no. 1, pp. 59–76, Jan. 2016.
[50] A. Giannitrapani, N. Ceccarelli, F. Scortecci, and A. Garulli, "Comparison of EKF and UKF for spacecraft localization via angle measurements," *IEEE Trans. Aerosp. Electron. Syst.*, vol. 47, no. 1, pp. 75–84, Jan. 2011.
[51] C. Yang, W. Shi, and W. Chen, "Comparison of unscented and extended Kalman filters with application in vehicle navigation," *J. Navigat.*, vol. 70, no. 2, pp. 411–431, Mar. 2017.
[52] K. Ahn and Y. Kang, "A particle filter localization method using 2D laser sensor measurements and road features for autonomous vehicle," *J. Adv. Transp.*, vol. 2019, pp. 1–11, Feb. 2019.
[53] M. Moreno-Cano, M. Zamora-Izquierdo, J. Santa, and A. F. Skarmeta, "An indoor localization system based on artificial neural networks and particle filters applied to intelligent buildings," *Neurocomputing*, vol. 122, pp. 116–125, Dec. 2013.

INAM ULLAH received the B.Sc. degree in electrical engineering (telecommunication) from the Department of Electrical Engineering, University of Science and Technology Bannu (USTB), KPK, Pakistan, in 2016, and the master's degree in information and communication engineering from the College of Internet of Things (IoT) Engineering, Hohai University (HHU), Changzhou Campus, China, in 2018, where he is currently pursuing the Ph.D. degree with the College of IoT Engineering. He was an Assistant Engineer with ZTE Islamabad, Pakistan, in 2016. His research interests include wireless sensor networks (WSNs), underwater sensor networks (USNs), the Internet of Things (IoT), antenna, and edge/fog computing. His awards and honors include the Best Student Award from USTB, in 2015, Top-10 students award of the College of Internet of Things (IoT) Engineering, in 2019 and Top-100 students award of Hohai University (HHU), in 2019.

YU SHEN is currently pursuing the degree with the College of Internet of Things (IoT) Engineering, Hohai University (HHU), Changzhou Campus, China. Her research interests include 5G systems, edge/fog computing, and underwater networks. She is a member of the Lab of Communications and Networks, Hohai University, under the supervision of Prof. XIN SU.

XIN SU (Senior Member, IEEE) received the B.E. degree in computer engineering from the Kunming University of Science and Technology, China, in 2008, the M.E. degree in computer engineering from Chosun University, South Korea, in 2010, and the Ph.D. degree from the Program in IT and Media Convergence Studies, Inha University, South Korea, in 2015. He is currently an Associate Professor with the College of Internet of Things (IoT) Engineering, Hohai University (HHU), Changzhou Campus, China. He focuses the research topics on mobile communication, 5G systems, edge computing/fog computing, the Internet of Things applications, and marine networks. Recent years, he has published more than 70 academic articles, including IEEE TII, FGCS, IEEE T-SUSC, IEEE CEM, and MONET. He currently works on the editorial board of IEEE Access and *Digital Communications and Networks*. He has served as the Organizer of International Conferences, such as IEEE CCNC, IEEE ISPA, ACM RACS, ACM SAC, and I-SPAN.

CHRISTIAN ESPOSITO graduated in computer engineering, in 2006, and received the Ph.D. degree, in 2009, both at the University of Naples "Federico II." He was an Assistant Professor with the University of Napoli "Federico II," and a two-year Research Fellow and a short-term Researcher with the Institute of High Performance Computing and Networking (ICAR) of the Italian National Research Council (CNR), from 2011 to 2015. He is currently a tenured Assistant Professor with the University of Salerno, and received the National Qualification in Italy as an Associate Professor in computer engineering and computer science, in May 2017 and July 2018, respectively. He has published about 80 articles both in international journals and conferences and has been a PC member or involved in the organization of about 60 international conferences/workshops. His interests include positioning systems, reliable and secure communications, and multi-objective optimization. He is a member of the Editorial Board of *International Journal of Computational Science and Engineering* and *International Journal of High Performance Computing and Networking*, both by Inderscience. He has served as a Guest Editor for special issues at multiple international journals. He is an Associate Editor of IEEE Access. He regularly serves as a Reviewer in journals and conferences in the field of distributed and dependable systems.

CHANG CHOI (Senior Member, IEEE) received the B.S., M.S., and Ph.D. degrees in computer engineering from Chosun University, in 2005, 2007, and 2012, respectively. He has been an Assistant Professor with Gachon University, since 2020. He has authored more than 50 publications, including articles in prestigious journals/conferences, such as the IEEE Communications Magazine, IEEE Transactions on Industrial Informatics, IEEE Transactions on Information Forensics and Security, IEEE Transactions on Sustainable Computing, IEEE Internet of Things Journal, *Information Sciences*, and *Future Generation Computer Systems*. His research interests include intelligent information processing, semantic web, smart IoT systems, and intelligent system security. He received the academic awards from the graduate school of Chosun University, in 2012. He also received a Korean government scholarship for graduate students (Ph.D. course), in 2008. He has served or is currently serving on the organizing or program committees of international conferences and workshops, such as ACM RACS, EAI BDTA, IE, ACM SAC, and IEEE CCNC/SeCHID. He has also served as a Guest Editor of high-profile journals, such as the IEEE Transactions on Industrial Informatics, *Future Generation Computer Systems*, *Applied Soft Computing*, *Multimedia Tools and Applications*, *Journal of Ambient Intelligence and Humanized Computing*, *Concurrency and Computation: Practice and Experience*, *Sensors*, and *Autosoft*.